



# Comparison of Subtyping Approaches and the Underlying Drivers of Microbial Signatures for Chronic Rhinosinusitis

Kristi Biswas,<sup>a</sup> Raewyn Cavubati,<sup>a</sup> Shan Gunaratna,<sup>a</sup> Michael Hoggard,<sup>b</sup> Sharon Waldvogel-Thurlow,<sup>a</sup> Jiwon Hong,<sup>a,b</sup> Kevin Chang,<sup>c</sup> Brett Wagner Mackenzie,<sup>a</sup> Michael W. Taylor,<sup>b</sup> Richard G. Douglas<sup>a</sup>

<sup>a</sup>Department of Surgery, The University of Auckland, Auckland, New Zealand

<sup>b</sup>School of Biological Science, Maurice Wilkins Centre for Molecular Biodiscovery, The University of Auckland, Auckland, New Zealand

<sup>c</sup>Department of Statistics, The University of Auckland, Auckland, New Zealand

**ABSTRACT** Chronic rhinosinusitis (CRS) is a heterogeneous condition characterized by persistent sinus inflammation and microbial dysbiosis. This study aimed to identify clinically relevant subgroups of CRS patients based on distinct microbial signatures, with a comparison to the commonly used phenotypic subgrouping approach. The underlying drivers of these distinct microbial clusters were also investigated, together with associations with epithelial barrier integrity. Sinus biopsy specimens were collected from CRS patients ( $n = 23$ ) and disease controls ( $n = 8$ ). The expression of 42 tight junction genes was evaluated using quantitative PCR together with microbiota analysis and immunohistochemistry for measuring mucosal integrity and inflammation. CRS patients clustered into two distinct microbial subgroups using probabilistic modelling Dirichlet (DC) multinomial mixtures. DC1 exhibited significantly reduced bacterial diversity and increased dispersion and was dominated by *Pseudomonas*, *Haemophilus*, and *Achromobacter*. DC2 had significantly elevated B cells and incidences of nasal polyps and higher numbers of *Anaerococcus*, *Megasphaera*, *Prevotella*, *Atopobium*, and *Propionibacterium*. In addition, each DC exhibited distinct tight junction gene and protein expression profiles compared with those of controls. Stratifying CRS patients based on clinical phenotypic subtypes (absence or presence of nasal polyps [CRSsNP or CRSwNP, respectively] or with cystic fibrosis [CRSwCF]) accounted for a larger proportion of the variation in the microbial data set than with DC groupings. However, no significant differences between CRSsNP and CRSwNP cohorts were observed for inflammatory markers, beta-dispersion, and alpha-diversity measures. In conclusion, both approaches used for stratifying CRS patients had benefits and pitfalls, but DC clustering provided greater resolution when studying tight junction impairment. Future studies in CRS should give careful consideration to the patient subtyping approach used.

**IMPORTANCE** Chronic rhinosinusitis (CRS) is a major human health problem that significantly reduces quality of life. While various microbes have been implicated, there is no clear understanding of the role they play in CRS pathogenesis. Another equally important observation made for CRS patients is that the epithelial barrier in the sinonasal cavity is defective. Finding a robust approach to subtype CRS patients would be the first step toward unravelling the pathogenesis of this heterogeneous condition. Previous work has explored stratification based on the clinical presentation of the disease (with or without polyps), inflammatory markers, pathology, or microbial composition. Comparisons between the different stratification approaches used in these studies have not been possible due to the different cohorts, analytical methods, or sample sites used. In this study, two approaches for subtyping CRS patients were compared, and the underlying drivers of the heterogeneity in CRS were also explored.

**Citation** Biswas K, Cavubati R, Gunaratna S, Hoggard M, Waldvogel-Thurlow S, Hong J, Chang K, Wagner Mackenzie B, Taylor MW, Douglas RG. 2019. Comparison of subtyping approaches and the underlying drivers of microbial signatures for chronic rhinosinusitis. *mSphere* 4:e00679-18. <https://doi.org/10.1128/mSphere.00679-18>.

**Editor** David W. Pascual, University of Florida

**Copyright** © 2019 Biswas et al. This is an open-access article distributed under the terms of the [Creative Commons Attribution 4.0 International license](https://creativecommons.org/licenses/by/4.0/).

Address correspondence to Richard G. Douglas, [Richard.douglas@auckland.ac.nz](mailto:Richard.douglas@auckland.ac.nz).

**Received** 6 December 2018

**Accepted** 12 December 2018

**Published** 6 February 2019

**KEYWORDS** epithelial barrier, microbiota, tight junctions, inflammation, mucosal integrity, sinusitis

As the first line of defense against inhaled antigens from the external environment, the upper airway epithelium represents an important physiological barrier (1). The close cell-to-cell proximity that is central to the integrity of this barrier is maintained by tight junctions, which play a critical role in host defense (2, 3). Tight junctions comprise a range of transmembrane and scaffolding adaptor proteins, including occludin, claudins, junctional adhesion molecules, and zonula occludens (ZO) (4). These proteins limit the passage of macromolecules by sealing off the paracellular spaces between epithelial cells. On the other hand, in cases of tissue inflammation, the opening of tight junctions assists in the release of tissue fluids and the influx of inflammatory cells, and by doing so, helps speed resolution. Accordingly, tight junctions are considered the gatekeepers of inflammatory disease.

Recent studies have considered the role of epithelial barrier defects in a number of chronic inflammatory conditions, including chronic rhinosinusitis (CRS) (5, 6). CRS is an inflammatory condition of the upper respiratory tract persisting for more than 12 weeks, affecting 5% of the general population (7). Symptoms include nasal discharge, facial pain, loss of smell, and headaches. CRS is a complex and heterogeneous disease with many underlying factors that present with similar symptoms, making it challenging to separate CRS into clinically relevant subtypes. Traditionally, the classification of CRS has been based on the clinical phenotypes, namely, the presence (CRSwNP) or absence (CRSSNP) of polyposis. Approximately 25% to 30% of CRS patients present with nasal polyps (8), and this cohort is considered to have a Th2-predominated inflammatory response, whereas patients with idiopathic CRS without nasal polyps (CRSSNP) have Th1-type responses. However, this simplified view misrepresents the true complexities of CRS.

Recent efforts have investigated the pathogenesis of CRS based on inflammatory markers (9, 10), microbiota composition (11, 12), pathology, or clinical factors (13, 14), but these studies have produced little consensus on appropriate strategies to subtype patients. The role of microbes in CRS remains unclear due to the frequent lack of resolution with antimicrobial treatment. It has been suggested that a loss of overall microbiota diversity and deleterious community changes (collectively termed dysbiosis) are more characteristic for CRS patients than a single disease-causing organism (15).

The stratification of patients based on probabilistic modeling of the bacterial communities in lower respiratory diseases, such as in patients with asthma and in HIV-infected patients with pneumonia, has been used successfully to classify immunological or clinical phenotypic variation across cohorts (16, 17). Using a similar approach, a recent study subtyped CRS patients based on their microbial community profiles (11). Each distinct microbial state was dominated by one bacterial family and associated with a unique clinical and host immune response. Previous studies have found that large interpersonal variations in the sinonasal microbiomes of CRS patients (subtyped based on clinical diagnosis) can make classification difficult (12). Accordingly, the distinct advantages of stratifying patients based on microbial community profiles are that it will help to resolve the microbial heterogeneity of CRS and that it is a step toward the implementation of a precision medicine approach. The underlying drivers of these distinct microbial states in CRS are yet to be investigated.

Several studies have investigated epithelial integrity in CRS mucosa and found that CRS patients with nasal polyps (CRSwNP) have severely disrupted epithelia with decreased expression of occludin and ZO-1 (6, 18, 19). These efforts also suggest a role for cytokines (gamma interferon [IFN- $\gamma$ ] and interleukin 4 [IL-4]) in disrupting tight junctions, whereas the influences of the microbes on the host are less understood.

One common hypothesis is that a loss of tight junction integrity in CRS patients could lead to the entry of environmental agents, including microbes, into host tissues (20). It remains unclear whether the microbes are the cause of tissue damage or if

microbial patterns or associations are the consequence of a leaky epithelium, leading to a buildup of microbial cells in the tissue. The mechanism by which bacteria penetrate the epithelial barrier is unknown, but their presence in CRS tissue (in particular, CRS with cystic fibrosis [CRSwCF]) presumably reflects a breakdown in mucosal integrity (21). Furthermore, any changes to the microenvironment (such as a lack of mucociliary clearance and damaged surfaces for bacterial cell adherence) could impact microbial composition and structure, as observed previously in gut studies (22).

In this study, we aimed to stratify CRS patients based on their microbial community compositions using a probabilistic modeling approach and the traditional phenotypic approach. In addition, we investigated several possible underlying influences on these microbial states by measuring gene and protein expressions of host tight junction, epithelial integrity, and inflammatory cells (T cells, B cells, and macrophages) in the sinonasal tissue biopsy specimens.

## RESULTS

**Clinical parameters.** Nonparametric pairwise comparisons were made based on clinical factors in this cohort of 31 subjects (CRS, 23; disease controls, 8).

Dirichlet multinomial mixtures using probabilistic modeling in R were used to stratify patients based on their microbial communities (operational taxonomic unit [OTU] level) (23). The Laplace approximation was used to find the model of best fit and determine the numbers of clusters from the data set. Unique microbial states were labeled Dirichlet clusters (DC).

None of the measured clinical factors were significantly different between the two DC groups (DC1 and DC2) and disease controls (data not shown). A similar analysis was performed on phenotypic subtypes of CRS (CRSsNP, CRSwNP, and CRSwCF) and disease controls (data not shown), where age and polyposis were found to be significant factors.

**Overall bacterial community composition.** Quality filtering resulted in 346,003 bacterial 16S rRNA gene sequences from 31 samples. Samples that did not meet a rarefaction threshold of 677 were removed from further analysis, including 3 CRSsNP samples. The final numbers of samples included in further analyses were 8 disease controls and 20 CRS patients (CRSsNP, 5; CRSwNP, 8; CRSwCF, 7; DC1, 13; DC2, 7). The final, rarefied data set included 200 taxonomically assigned OTUs at 97% sequence similarity (ranging from 4 to 45 OTUs per sample), and this OTU table was used for all subsequent microbial related analyses.

Large interpersonal variation in microbial community composition was observed between individuals of each cohort (Fig. 1). The bacterial taxa *Staphylococcus* (OTU2), *Streptococcus* (OTU7), *Propionibacterium* (OTU6), and *Corynebacteriaceae* (OTU10) were prevalent in a majority of the samples but only at low relative sequence abundances (Fig. 2A).

**Bacterial community compositions of DC groups.** Samples were assigned into clusters based on bacterial community composition using Dirichlet distributions (23). Dirichlet cluster 1 (DC1) comprised samples from all three CRS subgroups (CRSsNP, 4; CRSwNP, 2; CRSwCF, 7). In contrast, DC2 was dominated by CRSwNP samples ( $n = 6$ ) along with one CRSsNP sample.

A variety of alpha-diversity measurements revealed significant differences between DC1 and controls; however, no significant differences were noted between DC1 and DC2 and between DC2 and controls (Fig. 1B). The bacterial taxa *Pseudomonas* (average relative abundance  $\pm$  standard deviation [SD],  $19\% \pm 37\%$ ), *Achromobacter* ( $7.6\% \pm 27\%$ ), and *Haemophilus* ( $8.5\% \pm 27\%$ ) dominated DC1, while DC2 was dominated by *Moraxella* ( $18\% \pm 31.5\%$ ) and *Stenotrophomonas* ( $6.7\% \pm 17.7\%$ ); however, these taxa all had low prevalences, as shown in Fig. 2B. Interestingly, controls were not dominated by any single bacterial taxon but instead had a low abundance of multiple genera, some of which were highly prevalent.

Taxa that were significantly different between groups were investigated through multiple pairwise comparisons at OTU and genus levels (data not shown). OTUs with

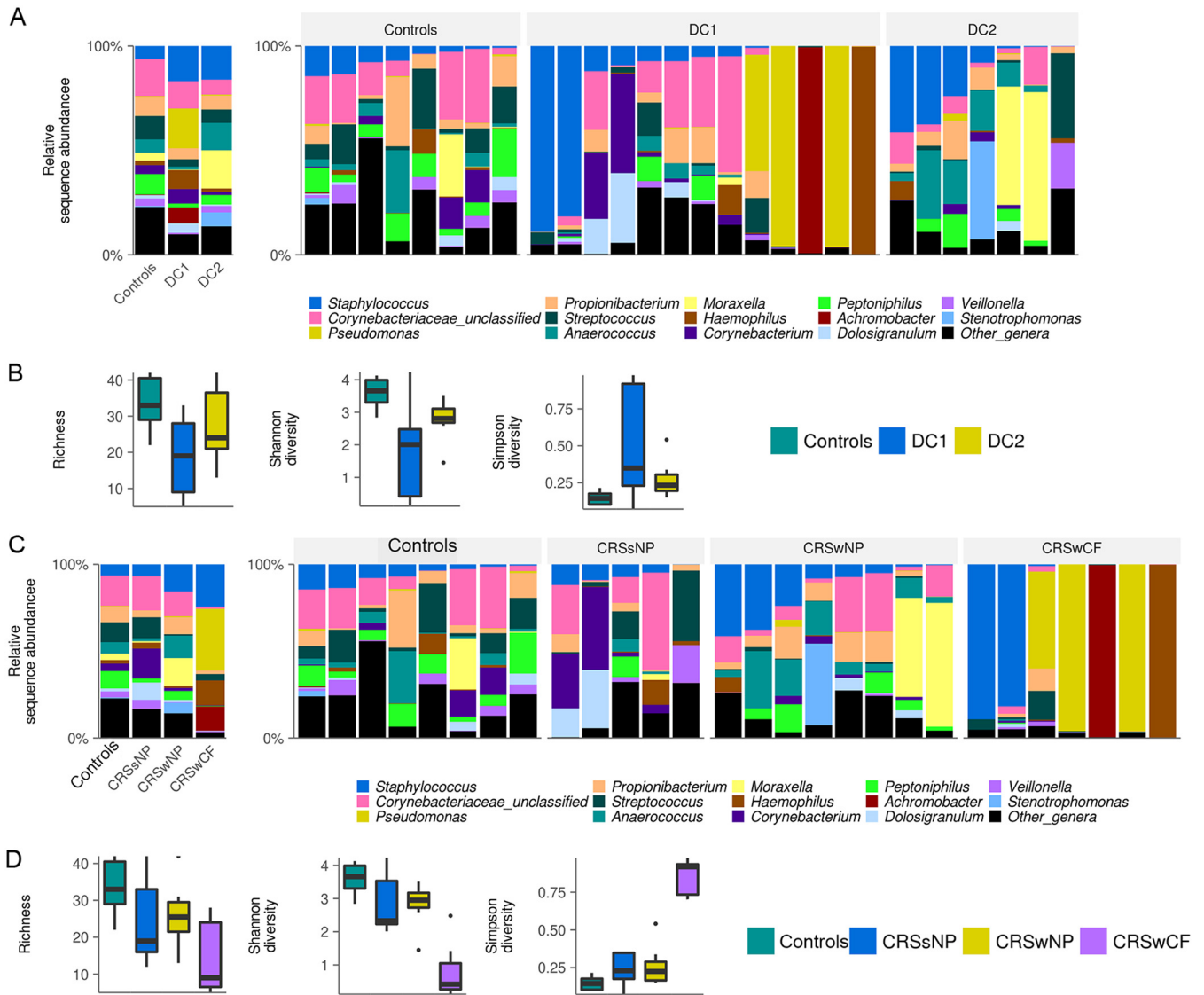


**FIG 1** Bacterial community composition and alpha diversity for the CRS cohorts and disease controls. Grouped and patient-level profiles at the genus level are shown in the bar graphs for DC groupings (A) and phenotypic groupings (C). Box-and-whisker plots represent group summaries for bacterial richness, Shannon diversity, and Simpson diversity for DC groupings (B) and phenotypic groupings (D). Horizontal lines represent significant differences ( $P < 0.05$ ) between cohorts.

significantly elevated abundance in DC2 compared with that in DC1 were *Anaerococcus* (OTU12, -19, and -251), *Prevotella* (OTU200), *Megasphaera* (OTU179), and *Atopobium* (OTU203). Control samples were differentiated from DC1 and DC2 by significant increases in *Streptococcus* (OTU7 and OTU18), *Veillonella* (OTU34), *Massilia* (OTU77), *Peptoniphilus* (OTU11), and *Halomonadaceae* (OTU109).

The dispersions of samples based on microbial community profiles in each DC were compared by calculating the distances to the centroid in nonmetric multidimensional scaling (nMDS) analyses. DC1 samples were significantly more dispersed than control samples ( $P = 0.011$ , Tukey's honest test) (Fig. 3B). In addition, a permutational multivariate analysis of variance (PERMANOVA) test confirmed that each of the clusters identified for the CRS cohort and control group explained a significant proportion ( $R^2 = 12.2\%$ ,  $P = 0.014$ ) of the overall variation in the bacterial data set. However, these PERMANOVA results should be interpreted with caution in light of the different beta-dispersion patterns of the groups assessed (24).

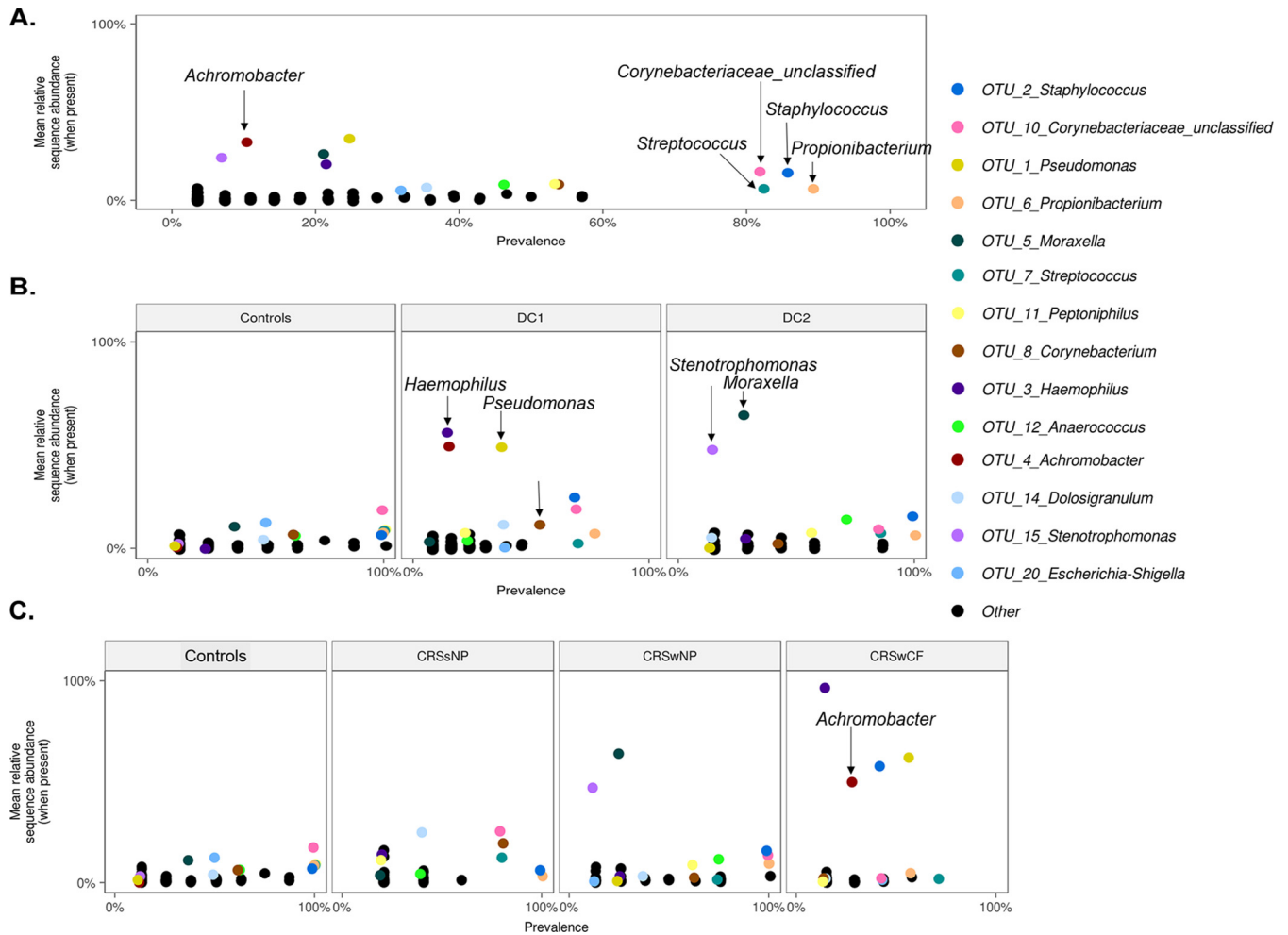


**FIG 2** Mean OTU relative abundances per sample (when present in a sample) plotted against prevalence (occurrence) across all samples (A), each DC and controls (B), and each phenotypic CRS subtype and controls (C). All OTUs are plotted. The 14 most abundant OTUs are color coded, and all other OTUs are presented as black dots.

**Bacterial community compositions of phenotypic groups.** Patients were also stratified based on clinical presentation of the disease, which includes the presence or absence of nasal polyposis and comorbidity of cystic fibrosis.

Alpha diversity was significantly ( $P < 0.001$ ) lower in CRSwCF patients than in controls. Significant differences in diversity were also observed ( $P < 0.05$ ) between CRSwCF and CRSwNP samples.

Similar to controls (as described above), CRSsNP did not show dominance of any single bacterial taxon. However, CRSwNP samples were dominated by *Moraxella* (average relative abundance  $\pm$  SD, 16%  $\pm$  30%) and *Stenotrophomonas* (5.8%  $\pm$  16.5%), while CRSwCF samples were dominated by *Pseudomonas* (35.4%  $\pm$  46%), *Staphylococcus* (24.5%  $\pm$  41.6%), *Achromobacter* (14.1%  $\pm$  37%), and *Haemophilus* (13.9%  $\pm$  36.8%) (Fig. 2C).

Pairwise comparisons between control samples and CRS subtypes (CRSsNP, CRSwNP, and CRSwCF) were performed on OTU- and genus-level data. CRSwCF samples were significantly reduced in *Propionibacterium*, *Corynebacterium*, *Anaerococcus*, and *Peptoniphilus* in comparison to controls. Furthermore, CRSsNP samples had a significantly lower abundance of *Peptoniphilus*, while CRSwNP samples had less *Streptococcus* and *Veillonella* than controls.

There were no significant differences in dispersion between phenotypic groups and controls according to an analysis of variance. However, PERMANOVA tests revealed that

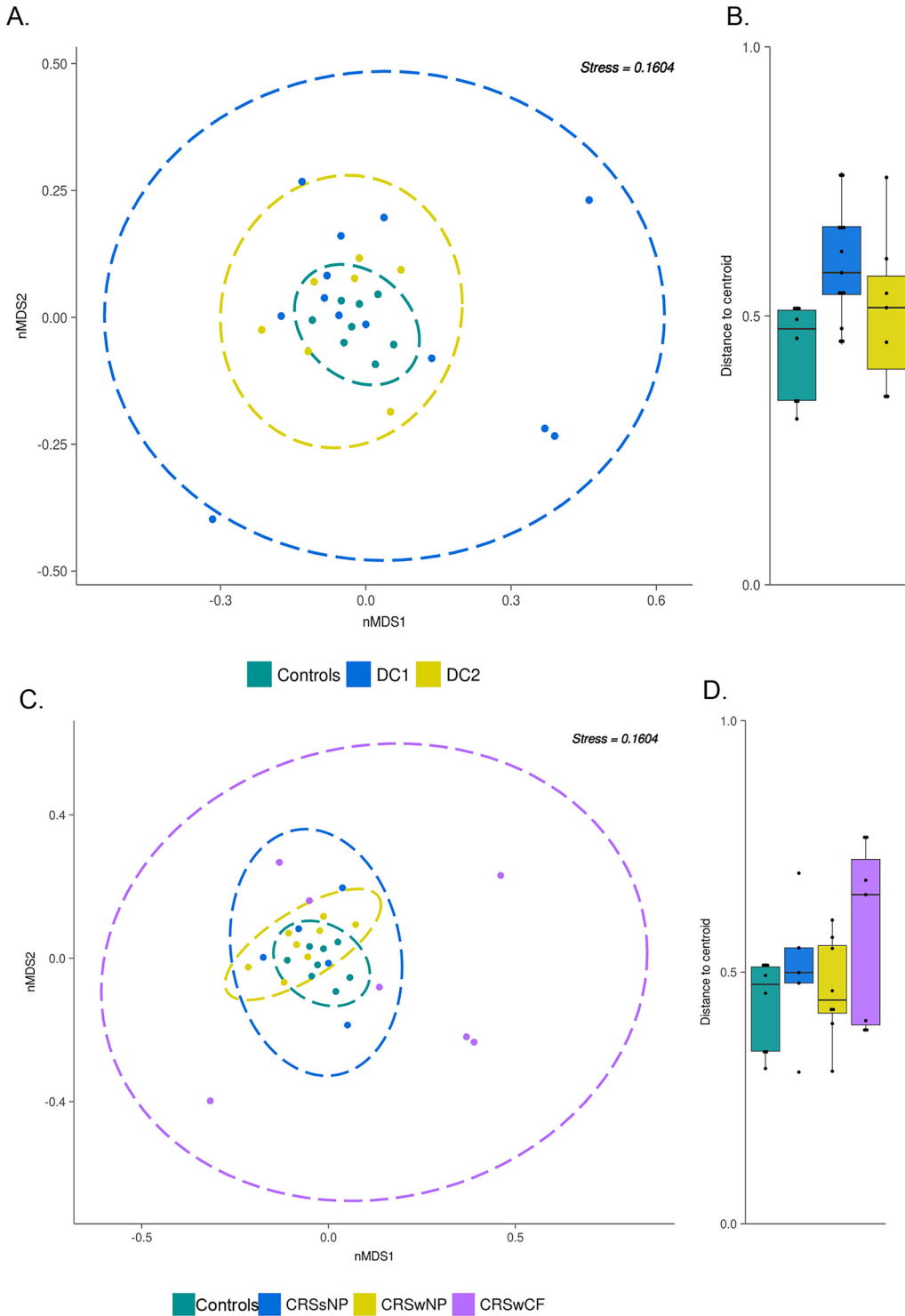


**FIG 3** Nonmetric multidimensional scaling plot using Bray-Curtis dissimilarity distances (weighted) for all samples for DC clustering (A) and phenotypic subtyping (C). Ellipses represent the 95% confidence interval (CI) spread from centroids. (B and D) Box-and-whisker plot of distances between each subject to the centroid of their respective groups. Beta-dispersion was significantly different between DC1 and controls ( $P = 0.0114$  by Tukey’s multiple comparisons of means).

phenotypic subtyping methods accounted for a larger proportion of the variation ( $R^2 = 23.4\%$ ,  $P = 0.001$ ) for CRS than DC clustering.

**Tight junction protein and gene expression patterns in sinonasal tissue.** Based on our initial aim to investigate the underlying drivers of each subtype in CRS, the

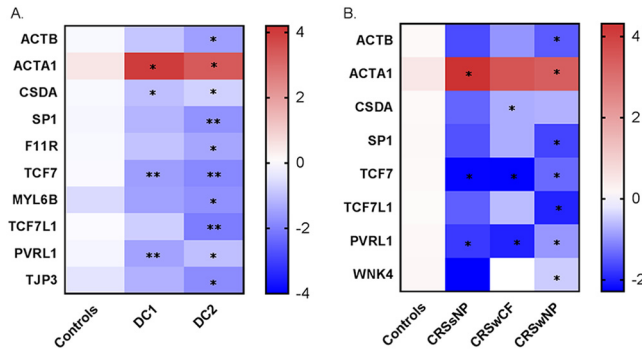


**FIG 4** Tight junction genes that were significantly different in expression for DC groups (A) and phenotypic subgroups (B) compared with that in controls are displayed in the heatmap. Blue represents genes that have low-level expression, and red represents higher expression. Values displayed are log transformed mean fold change ( $2^{-\Delta\Delta C_T}$ ). \*,  $P < 0.05$ ; \*\*,  $P < 0.01$ .

expression of 42 tight junction genes in sinonasal tissue biopsy specimens was measured for each patient and compared to that in disease controls. After results were normalized to a housekeeping gene, fold changes in gene expression were recorded for each DC and CRS phenotypic subtype compared to that for controls.

Ten tight junction genes were significantly under- or overexpressed in DC1 and/or DC2 compared to that in controls (Fig. 4A). The gene *ACTA1*, which encodes a skeletal  $\alpha$ -actin protein that maintains the cytoskeleton and cell movement, was the only gene to be significantly overexpressed in both DC1 and DC2. Each DC group exhibited unique tight junction gene expression patterns. Three genes were significantly underexpressed in DC1: *CSDA*, *TCF7*, and *PVRL1*. In DC2, nine genes were significantly underexpressed compared with the expression in the controls (Fig. 4A).

The subtyping patients on the basis of phenotypic characteristics revealed that 7 tight junction genes were underexpressed and the *ACTA1* was overexpressed in the CRS cohorts compared with that in the controls (Fig. 4B). Genes *PVRL1* and *TCF7* were significantly underexpressed in all three CRS subtypes. The expression profiles of CRSsNP and CRSwCF were very alike, with only one exception, gene *CSDA*, which was underexpressed in CRSwCF patients (Fig. 4B). A Spearman correlation analysis of the data set after adjusting for multiple comparisons showed a significant negative association between tight junction gene *MTDH* expression and members of the bacterial genus *Pseudomonas* (data not shown).

Staining of sinonasal tissue biopsy specimens identified ZO-1 and occludin proteins at apicolateral contact points of adjacent epithelial cells (data not shown). Claudin-1, by contrast, was predominantly seen in subapical regions, with concentrated continuous staining among the mid-basal regions of epithelial cells (data not shown). The staining area for ZO-1 was significantly ( $P = 0.03$ ) lower in DC2 (mean  $0.5\% \pm 0.3\%$ ) than in controls ( $1.1\% \pm 0.5\%$ ) (data not shown). There were no significant differences in claudin-1 and occludin staining in disease controls relative to that in DC1 and DC2. In addition, there were no significant differences in the staining for ZO-1, claudin-1, and occludin proteins in the three CRS subtypes compared with that in controls. Furthermore, no correlations were observed between tight junction proteins and the abundances of bacterial taxa (data not shown).

**Inflammatory state and mucosal integrity of tissue biopsy specimens.** Inflammatory marker cells (T cells, B cells, and macrophages) were enumerated in the tissue biopsy specimens to assess the inflammatory state of the patients. Although all three cell types were reduced in the disease controls compared with that in DC1 and DC2 cohorts, B cells ( $CD20^+$ ) were the only identified inflammatory marker with a significant difference between the groups, with higher numbers in DC2 (data not shown).

In contrast, by traditional CRS subtyping approaches, all three inflammatory marker cells were significantly elevated only in the CRSwNP cohort compared with that in

controls. There were no significant differences between the CRS subtype cohorts, except for the elevated amounts of macrophages (CD68<sup>+</sup>) in CRSwNP compared with that in CRSwCF.

The sinonasal tissue biopsy specimens were also assessed for mucosal integrity. Goblet cell enumeration and cilium integrity in the biopsy specimens were significantly reduced in DC2 compared with that in DC1 and control (data not shown). Similarly, when subtyping the same group of patients based on phenotypic approaches, goblet cell enumeration and cilium integrity were significantly reduced in CRSwNP patients compared with that in controls and CRSsNP patients. Interestingly, CRSwCF patients had no significant differences in mucosal integrity (collagen content, goblet cell enumeration, and cilium integrity) compared with that in controls. Furthermore, a Spearman correlation analysis showed a positive association between goblet cell counts and tight junction gene *LEF1* expression (data not shown). No other significant associations were found between mucosal integrity, inflammatory marker cells, and all other measured variables in this study.

## DISCUSSION

Endotyping of CRS patients has been the subject of considerable recent research, as it is hoped that a subclassification of this condition will allow for more specific and effective therapies to be administered. In this study, we defined microbial states for CRS using probabilistic modeling, in which patients with similar microbial states were clustered together. Furthermore, the same cohorts of patients were also subtyped based on phenotypic presentation of the disease. We then sought to understand the underlying influences on these cohorts by investigating sinonasal mucosal integrity, tight junction gene/protein expression, and inflammatory status. The two approaches of clustering CRS patients will be compared and discussed further.

**Resolving the microbial heterogeneity of CRS.** Phenotyping of CRS patients based on clinical factors can be subjective and provides little information about microbes and their involvement in this disease. As shown previously for gastrointestinal and lower and upper respiratory diseases (11, 16, 17, 23), distinct microbial states were identified for CRS patients, allowing for stratification based on bacterial composition. The advantage of the new clustering approach used in this study and by others (11) is that it reflects a patient's microbial state at the time and places the patient into a distinct microbial cluster type. Appropriate targeted treatment strategies could then be prescribed for patients in the future based on their distinct microbial pattern.

In this study, two distinct microbial states of CRS patients were identified that were significantly different in diversity, beta-dispersion, and the relative abundance of members from the genus *Anaerococcus*. Although this novel way of classifying CRS samples explained some of the microbial variations in the data set, there was still a large proportion of the variation that was not accounted for. This was most likely due to the sizeable interpatient variation observed in this study and reported previously (15, 25). We anticipate, with larger cohort sizes, these microbial states will be more pronounced and less obscured by individual variation. While studies that use less invasive approaches to obtain samples such as nasopharyngeal swabs and rinses are able to obtain larger cohort sizes (26, 27), these samples are not suitable for analyses of histology and mucosal integrity. In addition, tissue biopsy specimens are required to study host gene expression levels. For these reasons, tissue biopsy specimens were used in the analyses within this study.

Subtyping patients based on the phenotype of the disease (with or without nasal polyps or with cystic fibrosis) has been the most common approach to date. The results for the microbial communities from each of these subtypes confirm those previously described by our group (12, 25). Interestingly, a greater amount of the variation (23.4%) observed in the data set from this study was explained through this patient phenotypic clustering approach than by the DC approach.

**Potential drivers of microbial signatures for CRS patients.** An understanding of the underlying factors that shape the sinonasal microbial community of a CRS patient



is essential for defining the pathogenesis of this complex disease and for developing better treatment protocols. The most common hypothesis for the pathogenesis of CRS is that the epithelial barrier is defective (28). Allergens (such as pollen), host genetics, bacteria, viruses, or inflamed tissue could all contribute to the disruption of the sinonasal epithelial barrier (29). In this study, we chose to investigate several of these potential host factors that might contribute to CRS pathogenesis and determine their influence on the sinonasal microbial state. Of the 42 measured tight junction genes, 9 exhibited reduced expression in CRS patients compared with that in controls. Reduced expression of tight junction genes in CRS patients compared with that in controls was observed previously (6). The reason for the overexpression of *ACTA1*, which encodes a protein involved in cell motility, structure, and integrity (according to [www.uniprot.org](http://www.uniprot.org)), is unclear but presumably reflects the host's response to an impaired epithelial surface. Each DC in this study had a unique tight junction gene expression profile, suggesting that the two identified CRS DCs are functionally different. It remains unknown whether the expression of a specific tight junction gene could play a role in determining distinct microbial states in the nasal cavity, or vice versa. The significant association between tight junction genes and bacterial community compositions observed in this study needs further validation with *in vitro* tests. However, this observation provides some evidence of interactions between host tight junction gene expression and sinonasal microbial communities.

Stratification of patients based on the traditional phenotypic approach did not clearly separate the tight junction gene expression profiles of CRSsNP and CRSwCF cohorts. This lack of clarity suggests that future studies studying tight junction gene expression profiles in CRS patients should consider using alternative patient stratification approaches.

Of the three measured tight junction proteins in this study, only ZO-1 was significantly downregulated in DC2 relative to the expression in controls. ZO-1's adhesive function between transmembrane proteins and the underlying actin skeleton denotes its critical role at the epicenter of the tight junction complex (30, 31). Furthermore, depletion of ZO proteins in mammary epithelial cells results in the failure of tight junction strands to assemble and a consequent loss of barrier function (31). These findings suggest an important role for ZO-1 in the establishment of functioning tight junction complexes. It is possible that reduced expression of ZO-1 protein could underlie subsequent downregulation of integral tight junction proteins, resulting in a loss of barrier properties. A loss of claudin-4, ZO-1, occludin, and E-cadherin in tissue biopsy specimens of CRS patients was found previously (6, 32). The lack of any significant observations on the tight junction protein measurements in the phenotypic CRS subgroups compared with those in controls also emphasizes the need to look at other ways to stratify CRS.

Another potential driver of microbial states in CRS is mucosal integrity. Several studies have reported significant changes in the structure and composition of the mucosa in CRS (33–35). CRS subjects exhibited polarizing results regarding the evidence of mucus hypersecretion, with a significantly higher goblet cell count than in controls. Interestingly, DC2 cohorts had significantly lower goblet cell counts and reduced integrity of cilia than the DC1 cohort and controls. This observation was also made for subgroup CRSwNP patients in comparison to other CRS cohorts and controls. Mucociliary function in CRS is essential for the physiological function and immunity of the nose (36). A loss in function promotes the formation of biofilms and bacterial infections. Certain species of *Pseudomonas*, *Haemophilus*, and *Streptococcus* produce ciliostatic or ciliotoxic agents that could result in loss of ciliary function (37). In this study, correlations with cilium integrity, goblet cell numbers, and bacterial taxa were not observed. However, further research into toxin production by signature members of each cohort that results in cilium loss is required.

Previous studies have shown proinflammatory cytokines (IFN- $\gamma$  and IL-4) disrupt epithelial integrity *in vitro*, which in turn could cause changes to the sinonasal microenvironment by disrupting surfaces for attachment or increase the permeability of

microbes to the underlying tissue (6, 38). In addition, Cope et al. (11) found that distinct microbial clusters have unique patterns of immune response. Evidence from these studies suggests that microbial states are influenced by various host factors, possibly including cellular junctions. Furthermore, consistent with findings from other groups, CRS patients in this study based on microbial states (DC1 and DC2) or phenotypic subtyping (CRSwNP) had a higher abundance of B cells in the mucosa than the controls. Previous efforts have shown a proliferation of B cells in the sinonasal mucosa when exposed to antigens (39). Inflammatory cytokine IL-13 is a key factor in stimulating antibody production (such as IgE and IgA) by B cells in response to antigen exposure in airway inflammatory diseases (40). IgE levels are elevated in eosinophilic CRSwNP patients (41). Accordingly, the elevated level of B cells in CRS patients is a good indication of the inflammatory status of the sinonasal tissue of CRS patients.

**Stratification approach for CRS.** The traditional approach of stratifying CRS patients based on their phenotypic presentation of the disease is standard practice; however, such approaches do not unravel the complexities of the disease. This study showed that, while phenotypic subtyping approaches can help explain some of the variation in the microbial community data set, alternative methods using microbial signatures also have some benefits. Each microbial state of CRS in this study was found to have a unique tight junction expression profile, which was not observed with the phenotypic subtyping approach. Accordingly, it remains unclear whether microbial states influence, or are being influenced by, barrier impairment. To answer this question, *in vitro* studies will need to be undertaken in the future.

## MATERIALS AND METHODS

**Patient recruitment and sample collection.** Twenty-three adult patients undergoing functional endoscopic sinus surgery for CRS by a single surgeon (R.G.D.) were recruited for this study. Diagnosis and subsequent recruitment of CRS patients were based on EPOS 2012 guidelines (42). These included CRS patients with polyps (CRSwNP,  $n = 8$ ), CRS patients without polyps (CRSsNP,  $n = 8$ ), and CRS patients with cystic fibrosis (CRSwCF,  $n = 7$ ). Control subjects ( $n = 8$ ) without any signs of sinus disease undergoing endoscopic surgery for the removal of pituitary tumors or medial orbital decompression were also recruited. Control patients exhibited no evidence of mucosal inflammation on endoscopy or computed tomography scans. Exclusion criteria include an administration of systemic corticosteroids or antibiotics within 4 weeks prior to surgery, an age of  $<18$  years, immunodeficiency, pregnancy, and other comorbidities (apart from cystic fibrosis). This study was approved by the Health and Disability Ethics Committee of New Zealand (NTX/08/12/126). Prior to sample collection, informed written consent was obtained from all patients.

Patients completed a symptom score sheet, prior to surgery, in which the following CRS symptoms were rated on a scale of 0 to 5: nasal obstruction, anterior nasal discharge, posterior nasal discharge, facial pain or fullness, and loss of smell. These scores were summated to give the symptom severity score. Lund-Mackay scoring was used to quantify radiological disease severity (43). Tissue biopsy specimens were collected intraoperatively from the ethmoidal sinus under general anesthesia prior to the administration of topical vasoconstrictors or intravenous antibiotics. Biopsied specimens were rinsed in sterile saline and partitioned. Samples for quantitative PCR and bacterial community analysis were fixed in RNAlater for 24 h and then stored at  $-20^{\circ}\text{C}$ . Samples for immunohistochemistry analysis were fixed in Carnoy's solution (60% ethanol, 30% chloroform, and 10% glacial acetic acid) before paraffin embedding.

**Bacterial community analysis. (i) DNA extraction.** DNA was extracted from tissue biopsy specimens using sterile Lysing Matrix E bead tubes (MP Biomedicals, Australia) and the AllPrep DNA/RNA isolation kit (Qiagen, Germany) as previously described (44). A negative DNA extraction control using 200  $\mu\text{l}$  sterile water was carried out simultaneously.

**(ii) Bacterial community sequencing.** The V3-V4 region of the bacterial 16S rRNA gene was amplified using primers 341F and 806R (45), with Nextera DNA Library Prep kit adapters attached. PCRs, amplification conditions, and purifications were carried out as previously described (12). In brief, genomic DNA ( $\sim 100$  ng) from each sample was amplified in duplicate PCRs of 35 cycles and then pooled to a final volume of 50  $\mu\text{l}$ . Negative PCR controls were included in all PCRs and yielded no detectable amplicons. Eluent from the negative extraction control was also subjected to PCR amplification and yielded no detectable product. Purification using Agencourt AMPure magnetic beads (Beckman Coulter Inc., USA) was carried out as per the manufacturer's instructions. Purified PCR products were quantified using Qubit dsDNA High-Sensitivity kits (Life Technologies, New Zealand), standardized to  $\sim 5$  ng per sample, and submitted to the University of Auckland Genomics Centre for library preparation and sequencing using Illumina MiSeq ( $2 \times 300$  bp paired-end reads).

**(iii) Bioinformatics.** Sequences were merged and quality filtered in USEARCH (version 8.0) with default settings as previously described (12). OTU clustering based on a 97% 16S rRNA gene sequence similarity threshold was performed using the UCLUST algorithm in USEARCH (46). Each OTU was taxonomically assigned in QIIME (47) using the RDP classifier 2.2 against the SILVA 16S rRNA gene

database (version 128) (48, 49). Sequences mapping to the human genome were removed from subsequent analyses. Samples were rarefied to an even sequencing depth of 677 reads. Alpha diversity (including Shannon, Simpson, richness [observed OTUs]) and beta diversity (including weighted and unweighted UniFrac distances and Bray-Curtis dissimilarity) were calculated in QIIME. Graphical outputs were created in R (version 3.4.1) (50) and GraphPad Prism (version 7.03).

**RNA extraction and quantitative PCR.** RNA extraction of biopsied tissue was carried out in parallel with the DNA extraction using the AllPrep DNA/RNA isolation kit (Qiagen) as per the manufacturer's instructions. Extracted RNA was transferred to a collection tube and reelected in 30  $\mu$ l DNA/RNA-free sterile water.

Recovered RNA was treated with DNase I (Invitrogen) for selective degradation of contaminant DNA as per the manufacturer's instructions. The quantity and quality of RNA were measured using a NanoDrop 3000 spectrophotometer. Successful removal of genomic DNA from DNase-treated RNA samples was demonstrated by PCR targeting the human beta actin gene (51). DNase-treated RNA (standardized to  $\sim$ 100 ng/ $\mu$ l) was converted into cDNA using iScript<sup>TM</sup> Reverse Transcription Supermix for reverse transcriptase quantitative PCR (RT-qPCR; Bio-Rad, New Zealand) as per the manufacturer's instructions.

Pre-designed 384-well qPCR arrays (TJ H384) were obtained from Bio-Rad Laboratories Inc. (Auckland, New Zealand) for the analysis of 42 known tight junction genes and one housekeeping gene (*GAPDH*). Each sample was assessed for PCR performance, reverse transcription efficiency, DNA contamination, and RNA quality. Analysis of results was carried out using the ABI Prism 7900HT detection system (version 2.4). Each sample was run in duplicates on separate qPCR arrays and averaged for further analysis. Tight junction gene expression was normalized to the housekeeping gene *GAPDH*. The mean fold change of gene expression in CRS-affected patients compared to that in controls was calculated using the equation  $2^{-\Delta\Delta CT}$  (52).

**Histological analysis of sinonasal tissue.** Paraffin-embedded tissues were prepared into 4- $\mu$ m-thick sections and then mounted on Superfrost Plus positively charged microscope slides (Thermo Fisher Scientific).

**Statistical analysis.** Statistical analyses were carried out using GraphPad Prism software (CA, USA) and R. Dirichlet multinomial mixtures using probabilistic modeling in R was used to stratify patients based on their microbial communities (OUT level) (23). The Laplace approximation was used to find the model of best fit and determine the number of clusters from the data set. Unique microbial states were labeled Dirichlet clusters (DC). Sample dispersion between groups was compared using analysis of variance, permutation test (PERMDISP), and Tukey's honest significant differences in R. The software package adonis PERMANOVA using distance matrices (Bray-Curtis dissimilarity [weighted and unweighted] and UniFrac distances [weighted and unweighted]) was used to compare centroids of groups.

Multiple nonparametric pairwise comparisons for categorical variables (diagnosis, sex, ethnicity, polyposis, smoking status, antibiotic and steroid usage, and comorbidities) were tested using Fisher's exact test, with Bonferroni's adjustment for multiple comparisons. Pairwise comparisons between continuous variables for bacterial diversity, age, Lund-Mackay scores, symptom severity scores, tight junction gene expressions, histological analyses, bacterial OTUs, and genera were tested using Dunn's tests, with Bonferroni's adjustment for multiple comparisons. Heat maps depicting Spearman correlations, with significance calculated using Spearman coefficients, including multiple comparisons adjustment using the Benjamini and Hochberg false discovery rate (BH-FDR) with hierarchical clustering of correlation coefficients, were generated in R. Factors with significant ( $P < 0.05$ ) positive or negative correlations were plotted.

**Data availability.** Raw sequence reads were deposited into the SRA-NCBI database (BioProject identifier [ID] [PRJNA482256](https://doi.org/10.1016/j.tcb.2009.12.002), run numbers SRR8497507 to SRR8497537).

## ACKNOWLEDGMENTS

This work was supported by the Garnett Passe and Rodney Williams Memorial Foundation.

We declare no conflict of interest.

K.B., M.W.T., and R.G.D. contributed to the study design. K.B., R.C., S.G., M.H., S.W.-T., J.H., K.C., and B.W.M. contributed to data collection and analysis. K.B., R.C., M.W.T., and R.G.D. contributed to manuscript preparation.

## REFERENCES

1. Steed E, Balda MS, Matter K. 2010. Dynamics and functions of tight junctions. *Trends Cell Biol* 20:142–149. <https://doi.org/10.1016/j.tcb.2009.12.002>.
2. Förster C. 2008. Tight junctions and the modulation of barrier function in disease. *Histochem Cell Biol* 130:55–70. <https://doi.org/10.1007/s00418-008-0424-9>.
3. Kojima T, Go M, Takano K-i, Kurose M, Ohkuni T, Koizumi J-i, Kamekura R, Ogasawara N, Masaki T, Fuchimoto J, Obata K, Hirakawa S, Nomura K, Keira T, Miyata R, Fujii N, Tsutsumi H, Himi T, Sawada N. 2013. Regulation of tight junctions in upper airway epithelium. *Biomed Res Int* 2013: 947072. <https://doi.org/10.1155/2013/947072>.
4. Chiba H, Osanai M, Murata M, Kojima T, Sawada N. 2008. Transmembrane proteins of tight junctions. *Biochim Biophys Acta* 1778:588–600. <https://doi.org/10.1016/j.bbame.2007.08.017>.
5. Tieu DD, Kern RC, Schleimer RP. 2009. Alterations in epithelial barrier function and host defense responses in chronic rhinosinusitis. *J Allergy Clin Immunol* 124:37–42. <https://doi.org/10.1016/j.jaci.2009.04.045>.
6. Soyka MB, Wawrzyniak P, Eiwegger T, Holzmann D, Treis A, Wanke K,

- Kast JI, Akdis CA. 2012. Defective epithelial barrier in chronic rhinosinusitis: the regulation of tight junctions by IFN- $\gamma$  and IL-4. *J Allergy Clin Immunol* 130:1087.e10–1096.e10. <https://doi.org/10.1016/j.jaci.2012.05.052>.
7. Bhattacharyya N. 2003. The economic burden and symptom manifestations of chronic rhinosinusitis. *Am J Rhinol* 17:27–32. <https://doi.org/10.1177/194589240301700106>.
  8. Stevens WW, Schleimer RP, Kern RC. 2016. Chronic rhinosinusitis with nasal polyps. *J Allergy Clin Immunol Pract* 4:565–572. <https://doi.org/10.1016/j.jaip.2016.04.012>.
  9. Tomassen P, Vandeplas G, Van Zele T, Cardell L-O, Arebro J, Olze H, Förster-Ruhmann U, Kowalski ML, Olszewska-Zięber A, Holtappels G, De Ruyck N, Wang X, Van Drunen C, Mullol J, Hellings P, Hox V, Toskala E, Scadding G, Lund V, Zhang L, Fokkens W, Bachert C. 2016. Inflammatory endotypes of chronic rhinosinusitis based on cluster analysis of biomarkers. *J Allergy Clin Immunol* 137:1449.e4–1456.e4. <https://doi.org/10.1016/j.jaci.2015.12.1324>.
  10. Akdis CA, Bachert C, Cingi C, Dykewicz MS, Hellings PW, Naclerio RM, Schleimer RP, Ledford D. 2013. Endotypes and phenotypes of chronic rhinosinusitis: a PRACTALL document of the European Academy of Allergy and Clinical Immunology and the American Academy of Allergy, Asthma & Immunology. *J Allergy Clin Immunol* 131:1479–1490. <https://doi.org/10.1016/j.jaci.2013.02.036>.
  11. Cope EK, Goldberg AN, Pletcher SD, Lynch SV. 2017. Compositionally and functionally distinct sinus microbiota in chronic rhinosinusitis patients have immunological and clinically divergent consequences. *Microbiome* 5:53. <https://doi.org/10.1186/s40168-017-0266-6>.
  12. Hoggard M, Biswas K, Zoing M, Wagner Mackenzie B, Taylor MW, Douglas RG. 2017. Evidence of microbiota dysbiosis in chronic rhinosinusitis. *Int Forum Allergy Rhinol* 7:230–239. <https://doi.org/10.1002/alar.21871>.
  13. Tan NW, Cooksley CM, Roscioli E, Drilling AJ, Douglas R, Wormald PJ, Vreugde S. 2014. Small-colony variants and phenotype switching of intracellular *Staphylococcus aureus* in chronic rhinosinusitis. *Allergy* 69:1364–1371. <https://doi.org/10.1111/all.12457>.
  14. Lal D, Rounds AB, Rank MA, Divekar R. 2015. Clinical and 22-item sino-nasal outcome test symptom patterns in primary headache disorder patients presenting to otolaryngologists with “sinus” headaches, pain or pressure. *Int Forum Allergy Rhinol* 5:408–416. <https://doi.org/10.1002/alar.21502>.
  15. Wagner Mackenzie B, Waite DW, Hoggard M, Douglas RG, Taylor MW, Biswas K. 2017. Bacterial community collapse: a meta-analysis of the sinonasal microbiota in chronic rhinosinusitis. *Environ Microbiol* 19:381–392. <https://doi.org/10.1111/1462-2920.13632>.
  16. Teo SM, Mok D, Pham K, Kusel M, Serralha M, Troy N, Holt BJ, Hales BJ, Walker ML, Hollams E, Kochkov YA, Grindle K, Johnston SL, Gern JE, Sly PD, Holt PG, Holt KE, Inouye M. 2015. The infant nasopharyngeal microbiome impacts severity of lower respiratory infection and risk of asthma development. *Cell Host Microbe* 17:704–715. <https://doi.org/10.1016/j.chom.2015.03.008>.
  17. Shenoy MK, Iwai S, Lin DL, Worodria W, Ayakaka I, Byanyima P, Kaswabuli S, Fong S, Stone S, Chang E, Davis JL, Faruqi AA, Segal MR, Huang L, Lynch SV. 2017. Immune response and mortality risk relate to distinct lung microbiomes in patients with HIV and pneumonia. *Am J Respir Crit Care Med* 195:104–114. <https://doi.org/10.1164/rccm.201603-0523OC>.
  18. De Benedetto A, Rafaels NM, McGirt LY, Ivanov AI, Georas SN, Cheadle C, Berger AE, Zhang K, Vidyasagar S, Yoshida T, Boguniewicz M, Hata T, Schneider LC, Hanifin JM, Gallo RL, Novak N, Weidinger S, Beaty TH, Leung DYM, Barnes KC, Beck LA. 2011. Tight junction defects in patients with atopic dermatitis. *J Allergy Clin Immunol* 127:773.87–786.e7. <https://doi.org/10.1016/j.jaci.2010.10.018>.
  19. Lambrecht BN, Hammad H. 2012. The airway epithelium in asthma. *Nat Med* 18:684. <https://doi.org/10.1038/nm.2737>.
  20. Kim R, Freeman J, Waldvogel-Thurlow S, Roberts S, Douglas R. 2013. The characteristics of intramucosal bacteria in chronic rhinosinusitis: a prospective cross-sectional analysis. *Int Forum Allergy Rhinol* 3:349–354. <https://doi.org/10.1002/alar.21117>.
  21. Kim RJT, Park L, Wood AJ, Yin T, Jain R, Douglas RG. 2015. Chronic rhinosinusitis and cystic fibrosis: the interaction between sinus bacteria and mucosal immunity. *Int Forum Allergy Rhinol* 5:380–385. <https://doi.org/10.1002/alar.21431>.
  22. Tropini C, Earle KA, Huang KC, Sonnenburg JL. 2017. The gut microbiome: connecting spatial organization to function. *Cell Host Microbe* 21:433–442. <https://doi.org/10.1016/j.chom.2017.03.010>.
  23. Holmes I, Harris K, Quince C. 2012. Dirichlet multinomial mixtures: generative models for microbial metagenomics. *PLoS One* 7:e30126. <https://doi.org/10.1371/journal.pone.0030126>.
  24. Warton DJ, Wright ST, Wang Y. 2012. Distance-based multivariate analyses confound location and dispersion effects. *Methods Ecol Evol* 3:89–101. <https://doi.org/10.1111/j.2041-210X.2011.00127.x>.
  25. Biswas K, Hoggard M, Jain R, Taylor MW, Douglas RG. 2015. The nasal microbiota in health and disease: variation within and between subjects. *Front Microbiol* 6:134. <https://doi.org/10.3389/fmicb.2015.00134>.
  26. Chalermwatanachai T, Vilchez-Vargas R, Holtappels G, Lacoere T, Jáuregui R, Kerckhof F-M, Pieper DH, Van de Wiele T, Vaneechoutte M, Van Zele T, Bachert C. 2018. Chronic rhinosinusitis with nasal polyps is characterized by dysbacteriosis of the nasal microbiota. *Sci Rep* 8:7926. <https://doi.org/10.1038/s41598-018-26327-2>.
  27. Polzehl D, Weschta M, Podbielski A, Riechelmann H, Rimek D. 2005. Fungus culture and PCR in nasal lavage samples of patients with chronic rhinosinusitis. *J Med Microbiol* 54:31–37. <https://doi.org/10.1099/jmm.0.45881-0>.
  28. Lam K, Schleimer R, Kern RC. 2015. The etiology and pathogenesis of chronic rhinosinusitis: a review of current hypotheses. *Curr Allergy Asthma Rep* 15:41. <https://doi.org/10.1007/s11882-015-0540-2>.
  29. Yeo NK, Jang YJ. 2010. Rhinovirus infection-induced alteration of tight junction and adherens junction components in human nasal epithelial cells. *Laryngoscope* 120:346–352. <https://doi.org/10.1002/lary.20764>.
  30. Bauer H, Zweimueller-Mayer J, Steinbacher P, Lametschwandner A, Bauer HC. 2010. The dual role of zonula occludens (ZO) proteins. *J Biomed Biotechnol* 2010:402593. <https://doi.org/10.1155/2010/402593>.
  31. Fanning AS, Anderson JM. 2009. Zonula occludens-1 and-2 are cytosolic scaffolds that regulate the assembly of cellular junctions. *Ann N Y Acad Sci* 1165:113–120. <https://doi.org/10.1111/j.1749-6632.2009.04440.x>.
  32. Schleimer RP. 2017. Immunopathogenesis of chronic rhinosinusitis and nasal polyposis. *Annu Rev Pathol* 12:331–357. <https://doi.org/10.1146/annurev-pathol-052016-100401>.
  33. Yamauchi K, Inoue H. 2007. Airway remodeling in asthma and irreversible airflow limitation—ECM deposition in airway and possible therapy for remodeling. *Allergol Int* 56:321–329. <https://doi.org/10.2332/allergolint.R-07-151>.
  34. Van Bruaene N, Bachert C. 2011. Tissue remodeling in chronic rhinosinusitis. *Curr Opin Allergy Clin Immunol* 11:8–11. <https://doi.org/10.1097/ACI.0b013e32834233ef>.
  35. Ponikau JU, Sherris DA, Kephart GM, Kern EB, Gaffey TA, Tarara JE, Kita H. 2003. Features of airway remodeling and eosinophilic inflammation in chronic rhinosinusitis: is the histopathology similar to asthma? *J Allergy Clin Immunol* 112:877–882. <https://doi.org/10.1016/j.jaci.2003.08.009>.
  36. Cohen NA. 2006. Sinonasal mucociliary clearance in health and disease. *Ann Otol Rhinol Laryngol Suppl* 1196:20–26. <https://doi.org/10.1177/000348940611505904>.
  37. Gudis D, Zhao KQ, Cohen NA. 2012. Acquired cilia dysfunction in chronic rhinosinusitis. *Am J Rhinol Allergy* 26:1–6. <https://doi.org/10.2500/ajra.2012.26.3716>.
  38. Steelant B, Farré R, Wawrzyniak P, Belmans J, Dekimpe E, Vanheel H, Van Gerven L, Kortekaas Krohn I, Bullens DMA, Ceuppens JL, Akdis CA, Boeckxstaens G, Seys SF, Hellings PW. 2016. Impaired barrier function in patients with house dust mite-induced allergic rhinitis is accompanied by decreased occludin and zonula occludens-1 expression. *J Allergy Clin Immunol* 137:1043.e5–1053.e5. <https://doi.org/10.1016/j.jaci.2015.10.050>.
  39. Kato A. 2015. Immunopathology of chronic rhinosinusitis. *Allergol Int* 64:121–130. <https://doi.org/10.1016/j.alit.2014.12.006>.
  40. Kato A, Hulse KE, Tan BK, Schleimer RP. 2013. B-lymphocyte lineage cells and the respiratory system. *J Allergy Clin Immunol* 131:933–957. <https://doi.org/10.1016/j.jaci.2013.02.023>.
  41. Gevaert P, Nouri-Aria KT, Wu H, Harper CE, Takhar P, Fear DJ, Acke F, De Ruyck N, Banfield G, Kariyawasam HH, Bachert C, Durham SR, Gould HJ. 2013. Local receptor revision and class switching to IgE in chronic rhinosinusitis with nasal polyps. *Allergy* 68:55–63. <https://doi.org/10.1111/all.12054>.
  42. Fokkens WJ, Lund VJ, Mullol J, Bachert C, Alobid I, Baroody F, Cohen N, Cervin A, Douglas G, Gevaert P, Georgalas C, Goossens H, Harvey R, Hellings P, Hopkins C, Jones N, Joos G, Kalogjera L, Kern B, Kowalski M, Price D, Riechelmann H, Schlosser R, Senior B, Thomas M, Toskala E, Voegels R, Wang DY, Wormald PJ. 2012. EPOS 2012: European position paper on rhinosinusitis and nasal polyps 2012. A summary for otorhinolaryngologists. *Rhinology* 50:1–12. <https://doi.org/10.4193/Rhino50E2>.
  43. Hopkins C, Browne JP, Slack R, Lund V, Brown P. 2007. The Lund-Mackay staging system for chronic rhinosinusitis: how is it used and what does

- it predict? *Otolaryngol Head Neck Surg* 137:555–561. <https://doi.org/10.1016/j.otohns.2007.02.004>.
44. Kim RJT, Biswas K, Hoggard M, Taylor MW, Douglas RG. 2015. Paired analysis of the microbiota of surface mucus and whole-tissue specimens in patients with chronic rhinosinusitis. *Int Forum Allergy Rhinol* 5:877–883. <https://doi.org/10.1002/alr.21600>.
  45. Herlemann DPR, Labrenz M, Jürgens K, Bertilsson S, Waniek JJ, Andersson AF. 2011. Transitions in bacterial communities along the 2000 km salinity gradient of the Baltic Sea. *ISME J* 5:1571. <https://doi.org/10.1038/ismej.2011.41>.
  46. Edgar RC. 2010. Search and clustering orders of magnitude faster than BLAST. *Bioinformatics* 26:2460–2461. <https://doi.org/10.1093/bioinformatics/btq461>.
  47. Caporaso JG, Kuczynski J, Stombaugh J, Bittinger K, Bushman FD, Costello EK, Fierer N, Peña AG, Goodrich JK, Gordon JI, Huttley GA, Kelley ST, Knights D, Koenig JE, Ley RE, Lozupone CA, McDonald D, Muegge BD, Pirrung M, Reeder J, Sevinsky JR, Turnbaugh PJ, Walters WA, Widmann J, Yatsunenko T, Zaneveld J, Knight R. 2010. QIIME allows analysis of high-throughput community sequencing data. *Nat Methods* 7:335. <https://doi.org/10.1038/nmeth.f.303>.
  48. Quast C, Pruesse E, Yilmaz P, Gerken J, Schweer T, Yarza P, Peplies J, Glöckner FO. 2013. The SILVA ribosomal RNA gene database project: improved data processing and web-based tools. *Nucleic Acids Res* 41: D590–D596. <https://doi.org/10.1093/nar/gks1219>.
  49. Wang Q, Garrity GM, Tiedje JM, Cole JR. 2007. Naive Bayesian classifier for rapid assignment of rRNA sequences into the new bacterial taxonomy. *Appl Environ Microbiol* 73:5261–5267. <https://doi.org/10.1128/AEM.00062-07>.
  50. R Core Team. 2015. R: a language and environment for statistical computing. R Foundation for Statistical Computing, Vienna, Austria.
  51. Wang X, Seed B. 2003. A PCR primer bank for quantitative gene expression analysis. *Nucleic Acids Res* 31:e154. <https://doi.org/10.1093/nar/gng154>.
  52. Livak KJ, Schmittgen TD. 2001. Analysis of relative gene expression data using real-time quantitative PCR and the  $2^{-\Delta\Delta CT}$  method. *Methods* 25:402–408. <https://doi.org/10.1006/meth.2001.1262>.